

V_{us} and neutron beta decay

A. García

Departamento de Física, Centro de Investigación y de Estudios Avanzados del Instituto Politécnico Nacional, Apartado Postal 14-740, México, Distrito Federal, 07000, Mexico

G. Sánchez-Colón*

Departamento de Física Aplicada, Centro de Investigación y de Estudios Avanzados del Instituto Politécnico Nacional, Unidad Mérida, Apartado Postal 73, Cordemex, Mérida, Yucatán, 97310, Mexico

(Received 21 November 2007; published 11 April 2008)

We discuss the effect of the recent change of V_{us} by 3 standard deviations on the standard model predictions for neutron beta decay observables. We also discuss the effect the experimental error bars of V_{us} have on such predictions. Refined precision tests of the standard model will be made by a combined effort to improve measurements in neutron beta decay and in strangeness-changing decays. By itself the former will yield very precise measurements of V_{ud} and also make very precise predictions for V_{us} .

DOI: [10.1103/PhysRevD.77.073005](https://doi.org/10.1103/PhysRevD.77.073005)

PACS numbers: 12.15.Hh, 13.30.Ce, 14.20.Dh

I. INTRODUCTION

The precision measurements of the decay rate R and the electron-asymmetry α_e in neutron beta decay ($n\beta d$) [1] and their further improvements in the near future provide an excellent opportunity to test the standard model (SM) [2] and even to establish deviations signaling new physics. However, the predictions for these observables are afflicted by our current inability to compute reliably the Cabibbo-Kobayashi-Maskawa (CKM) matrix element V_{ud} and the leading form factor ratio $\lambda = g_1/f_1$. Both are better handled as free parameters to be determined from experiment. The theoretical predictions are then confined to a region in the (α_e, R) plane or equivalently in the (λ, R) plane where the SM is expected to remain valid within a certain confidence level (CL), say 90%. This region may be referred to as the standard model region (SMR). At first, it may look as if the predictions of the SM are severely limited by the experimental situation of R and α_e . However, this is not the case.

In a previous paper [3] we showed that the SMR is determined by the validity of the formulas predicted by the SM for the observables in $n\beta d$ and of the CKM unitarity. The size of the SMR depends on the theoretical uncertainties of such formulas and the experimental values of V_{us} and V_{ub} . Since such uncertainties in R and α_e are substantially smaller than their experimental error bars, a much more narrow SMR can be predicted even when V_{ud} and λ remain as free parameters. The predictions of SM are then greatly improved, and it is these that are meaningful to compare with the measured R and α_e .

Nevertheless, such predictions are indeed affected by the experimental values of V_{ub} and V_{us} . The former is quite precise already, and its changes do not produce perceptible changes in the SMR. However, changes in V_{us} do produce important changes in the position and size of the SMR. It is

the purpose of this paper to extend the analysis of Ref. [3] and discuss the dependence of the SMR on the value of V_{us} . This has become more pressing since recently [1] its experimental value increased by 3 standard deviations from the value available for the analysis of [3].

In Sec. II we shall review the SM formulas for $n\beta d$ observables and the method to determine the predicted SMR. In Sec. III we shall determine the changes in the SMR corresponding to the new value of V_{us} . We shall also determine its position allowing for variations of up to 3 standard deviations of the present V_{us} . The role of V_{us} has another aspect: its precision significantly affects the size of the SMR. This will be studied in Sec. IV. A complementary analysis comes from the fact that precise measurements of R and α_e will produce a precise determination of V_{ud} . Assuming the validity of the unitarity of the CKM matrix, then $n\beta d$ can make quite precise predictions for V_{us} . We shall go into them in Sec. V. The last section is reserved for discussion and conclusions.

II. DETERMINATION OF THE STANDARD MODEL REGION

The SM predicts for the decay rate of $n\beta d$ the expression

$$R(10^{-3} \text{ s}^{-1}) = |V_{ud}|^2(0.1897)(1 + 3\lambda^2) \times (1 + 0.0739 \pm 0.0008) \quad (1)$$

at the level of a precision of 10^{-4} . V_{ud} and λ appear as free parameters. The detailed derivation of Eq. (1) is found in Ref. [4]. The main source of uncertainty in (1) is the model dependence of the contributions of Z^0 to the radiative corrections. A very conservative estimate is ± 0.0008 [5]. If one assumes dominance of the A_1 resonance [6], this uncertainty becomes the uncertainty of such an approximation, and then in Eq. (1) it can be estimated to be somewhat less than ± 0.0002 . Other uncertainties as in the values of the induced weak magnetism and pseudoten-

*gsanchez@mda.cinvestav.mx

sor form factors can be shown to contribute to 10^{-5} or less. Equation (1) has also been discussed in Ref. [7], where it was referred to as the master formula. Although presented in a somewhat different form, one can readily verify that the result of this reference confirms Eq. (1).

At the 10^{-4} level the SM predicts for the electron asymmetry the expression [8]

$$\alpha_e = \frac{-0.2089 \times 10^{-3} - 0.2763\lambda - 0.2772\lambda^2}{0.1897 + 0.5692\lambda^2}. \quad (2)$$

We have chosen a negative sign for λ to conform with the convention of [1]. The important remark here is that there is no theoretical uncertainty in α_e at this level of precision. The reason for this is that the uncertainty introduced by Z^0 is common to the numerator and denominator of α_e and cancels away at the 10^{-4} level. It must be stressed that α_e depends only on λ so that the experimental determination of λ is independent of V_{ud} .

The analysis that leads to Eq. (2) can be extended to the neutrino and electron-neutrino asymmetry coefficients. We shall not go further into this because it has remained customary to present experimental results for the old order zero angular coefficients [1],

$$B_0 = \frac{2\lambda(\lambda - 1)}{1 + 3\lambda^2}, \quad (3)$$

$$a_0 = \frac{1 - \lambda^2}{1 + 3\lambda^2}. \quad (4)$$

Also, instead of presenting results for α_e it is customary to give directly the value for λ , after all corrections contained in α_e have been applied to the experimental analysis. Thus, the relevance of exhibiting Eq. (2) is to show that the experimental value of λ is free of theoretical uncertainties at the 10^{-4} level.

Another very important constraint for our work here is the unitarity of the CKM matrix, which we shall use in the form

$$V_{ub} = \sqrt{1 - V_{ud}^2 - V_{us}^2}. \quad (5)$$

Given the experimental values of V_{ub} and V_{us} , the only free parameter in Eq. (5) is V_{ud} .

The current experimental situation [1] for Eqs. (1) and (3)–(5) is given by $R = 1.129\,05(102) \times 10^{-3} \text{ s}^{-1}$, $B_0 = 0.981(4)$, $a_0 = -0.103(4)$, $V_{ub} = 0.004\,31(30)$, and $V_{us} = 0.2257(21)$. It is this last number that recently increased by 3 standard deviations from its previous value and whose effect on the SMR we are going to determine. The experimental situation of λ is at present ambiguous. Its four more precise determinations are $\lambda_A = -1.2739(19)$ [9], $\lambda_L = -1.266(4)$ [10], $\lambda_Y = -1.2594(38)$ [11], and $\lambda_B = -1.262(5)$ [12]. The last three are statistically compatible and produce an average $\lambda_{LYB} = -1.2624(24)$. This average is not statistically compatible with the value λ_A . Although one may quote an average of the four $\lambda_{ALYB} =$

$-1.2695(15)$, one must remember that such an average is not a consistent one. Even so, it will still be interesting to discuss it.

To determine the SMR we shall form a χ^2 function with the six constraints Eqs. (1) and (3)–(5), V_{ub}^{exp} , and V_{us}^{exp} . This is an overconstrained system of restrictions for three free parameters: λ , V_{ud} , and V_{us} . This function is

$$\chi^2 = \left(\frac{R' - R}{\sigma_{R'}}\right)^2 + \left(\frac{\lambda' - \lambda}{\sigma_{\lambda'}}\right)^2 + \left(\frac{B_0^{\text{exp}} - B_0}{\sigma_{B_0}}\right)^2 + \left(\frac{a_0^{\text{exp}} - a_0}{\sigma_{a_0}}\right)^2 + \left(\frac{V_{ub}^{\text{exp}} - V_{ub}}{\sigma_{V_{ub}}}\right)^2 + \left(\frac{V_{us}^{\text{exp}} - V_{us}}{\sigma_{V_{us}}}\right)^2. \quad (6)$$

The SMR is determined by minimizing χ^2 at a fine lattice of points (λ', R') in the (λ, R) plane. It will correspond to the 90% CL region in this plane. That is, within this region the SM may be expected to remain valid at the 90% CL.

The key element in the determination of the SMR is that $\sigma_{R'}$ and $\sigma_{\lambda'}$ are not limited to take their current experimental values $\sigma_R = 0.001\,02 \times 10^{-3} \text{ s}^{-1}$ and σ_λ around 0.0024. We are at liberty to reduce them down to their theoretical uncertainty, namely, a few parts at 10^{-4} . The theoretically predicted SMR will correspond to $\sigma_{R'}$ and $\sigma_{\lambda'}$ at approximately one-tenth of their current experimental counterparts.

TABLE I. The minimum of χ^2 (χ_0^2) and its corresponding value of λ (λ_0) for seven values of R (which change in steps of one σ_R). In each row the upper, middle, and lower entries correspond to the size of error bars of R and λ discussed in the text. The 90% CL ranges for λ are displayed in the last column. V_{us} is assumed to be at $V_{us}^{\text{exp}} - 3\sigma_{V_{us}}$, with $\sigma_{V_{us}} = 0.0021$.

R'	χ_0^2	λ_0	λ'
1.125 09	2.974 56	-1.265 22	(-1.269 61, -1.260 85)
	2.974 95	-1.265 21	(-1.266 50, -1.263 93)
	2.974 96	-1.265 21	(-1.266 43, -1.264 00)
1.126 41	2.939 35	-1.266 12	(-1.270 49, -1.261 74)
	2.939 58	-1.266 10	(-1.267 40, -1.264 83)
	2.939 58	-1.266 10	(-1.267 33, -1.264 90)
1.127 73	2.913 57	-1.267 00	(-1.271 38, -1.262 63)
	2.913 68	-1.266 99	(-1.268 29, -1.265 72)
	2.913 68	-1.266 99	(-1.268 22, -1.265 79)
1.129 05	2.897 15	-1.267 89	(-1.272 27, -1.263 51)
	2.897 19	-1.267 89	(-1.269 18, -1.266 61)
	2.897 19	-1.267 89	(-1.269 11, -1.266 68)
1.130 37	2.890 05	-1.268 78	(-1.273 16, -1.264 40)
	2.890 05	-1.268 78	(-1.270 08, -1.267 50)
	2.890 05	-1.268 78	(-1.270 01, -1.267 57)
1.131 69	2.892 20	-1.269 67	(-1.274 05, -1.265 29)
	2.892 21	-1.269 67	(-1.270 97, -1.268 39)
	2.892 21	-1.269 67	(-1.270 90, -1.268 46)
1.133 01	2.903 53	-1.270 55	(-1.274 93, -1.266 18)
	2.903 60	-1.270 56	(-1.271 86, -1.269 28)
	2.903 60	-1.270 56	(-1.271 79, -1.269 35)

TABLE II. The minimum of χ^2 (χ_0^2) and its corresponding value of λ (λ_0) for seven values of R (which change in steps of one σ_R). In each row the upper, middle, and lower entries correspond to the size of error bars of R and λ discussed in the text. The 90% CL ranges for λ are displayed in the last column. V_{us} is assumed to be at V_{us}^{exp} , with $\sigma_{V_{us}} = 0.0021$.

R'	χ_0^2	λ_0	λ'
1.125 09	2.903 89	-1.267 46	(-1.271 86, -1.263 08)
	2.903 96	-1.267 46	(-1.268 79, -1.266 14)
	2.903 96	-1.267 46	(-1.268 72, -1.266 21)
1.126 41	2.892 29	-1.268 35	(-1.272 75, -1.263 96)
	2.892 30	-1.268 35	(-1.269 69, -1.267 04)
	2.892 30	-1.268 35	(-1.269 62, -1.267 11)
1.127 73	2.890 03	-1.269 24	(-1.273 64, -1.264 86)
	2.890 03	-1.269 25	(-1.270 58, -1.267 93)
	2.890 03	-1.269 25	(-1.270 51, -1.268 00)
1.129 05	2.897 03	-1.270 13	(-1.274 52, -1.265 75)
	2.897 07	-1.270 14	(-1.271 47, -1.268 82)
	2.897 07	-1.270 14	(-1.271 40, -1.268 89)
1.130 37	2.913 25	-1.271 02	(-1.275 41, -1.266 63)
	2.913 36	-1.271 03	(-1.272 37, -1.269 72)
	2.913 36	-1.271 03	(-1.272 30, -1.269 78)
1.131 69	2.938 62	-1.271 91	(-1.276 30, -1.267 52)
	2.938 84	-1.271 92	(-1.273 26, -1.270 61)
	2.938 84	-1.271 92	(-1.273 17, -1.270 68)
1.133 01	2.973 09	-1.272 80	(-1.277 19, -1.268 41)
	2.973 47	-1.272 81	(-1.274 15, -1.271 50)
	2.973 47	-1.272 81	(-1.274 08, -1.271 57)

TABLE III. The minimum of χ^2 (χ_0^2) and its corresponding value of λ (λ_0) for seven values of R (which change in steps of one σ_R). In each row the upper, middle, and lower entries correspond to the size of error bars of R and λ discussed in the text. The 90% CL ranges for λ are displayed in the last column. V_{us} is assumed to be at $V_{us}^{\text{exp}} + 3\sigma_{V_{us}}$, with $\sigma_{V_{us}} = 0.0021$.

R'	χ_0^2	λ_0	λ'
1.125 09	2.893 10	-1.269 77	(-1.274 18, -1.265 37)
	2.893 12	-1.269 78	(-1.271 15, -1.268 43)
	2.893 12	-1.269 78	(-1.271 09, -1.268 50)
1.126 41	2.905 67	-1.270 67	(-1.275 07, -1.266 27)
	2.905 74	-1.270 68	(-1.272 05, -1.269 32)
	2.905 74	-1.270 68	(-1.271 98, -1.269 39)
1.127 73	2.927 46	-1.271 56	(-1.275 96, -1.267 15)
	2.927 64	-1.271 57	(-1.272 94, -1.270 22)
	2.927 64	-1.271 57	(-1.272 88, -1.270 29)
1.129 05	2.958 43	-1.272 45	(-1.276 85, -1.268 05)
	2.958 75	-1.272 46	(-1.273 84, -1.271 11)
	2.958 75	-1.272 46	(-1.273 77, -1.271 18)
1.130 37	2.998 52	-1.273 34	(-1.277 74, -1.268 94)
	2.999 01	-1.273 36	(-1.274 73, -1.272 00)
	2.999 02	-1.273 36	(-1.274 67, -1.272 07)
1.131 69	3.047 66	-1.274 22	(-1.278 63, -1.269 83)
	3.048 37	-1.274 25	(-1.275 62, -1.272 90)
	3.048 38	-1.274 25	(-1.275 56, -1.272 96)
1.133 01	3.105 80	-1.275 11	(-1.279 52, -1.270 71)
	3.106 77	-1.275 14	(-1.276 52, -1.273 79)
	3.106 78	-1.275 14	(-1.276 45, -1.273 86)

In the next two sections we shall study the effects of V_{us} on the determination of the SMR. Its central value will affect its position in the (λ, R) plane, and its error bar will affect its width.

III. V_{us} AND THE STANDARD MODEL REGION

We shall work within a rectangle of the (λ, R) plane. The side for λ will be $(-1.2744, -1.2552)$ due to the ambiguity of the experimental value of λ [13]. We shall fold by quadratures the theoretical uncertainty of R into its experimental error bar to get an effective $\sigma_R = 0.00132 \times 10^{-3} \text{ s}^{-1}$. The other side of the rectangle will cover three

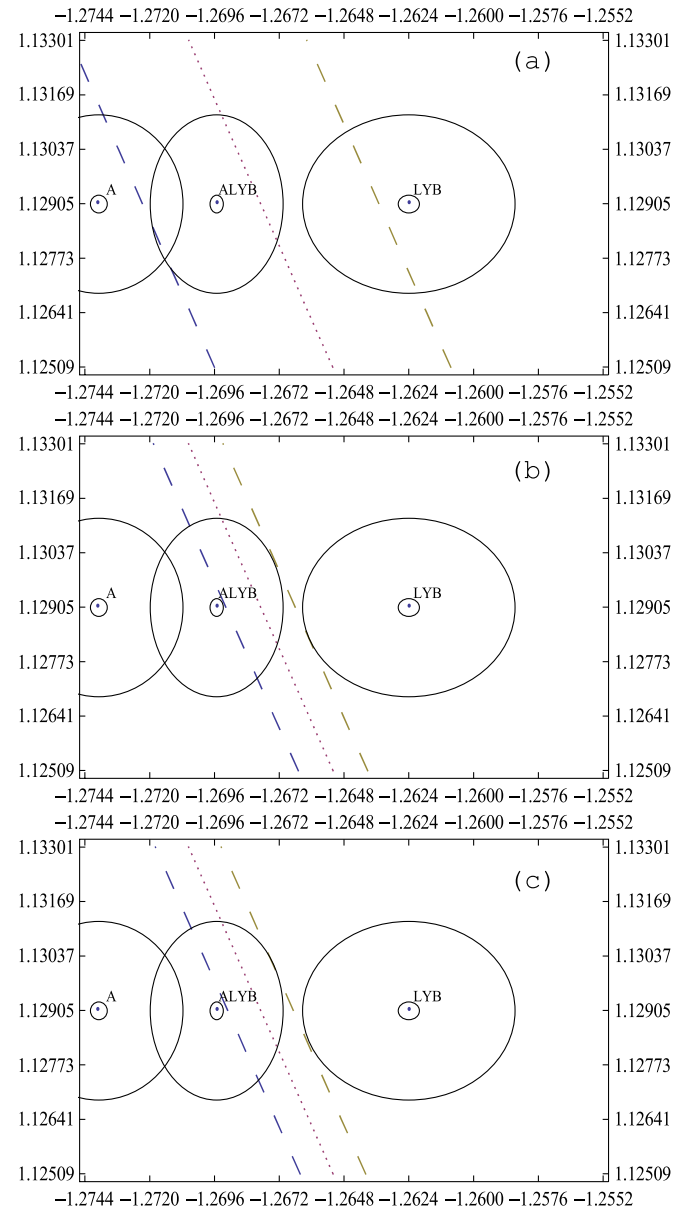


FIG. 1 (color online). The detailed numerical results corresponding to Table I are plotted here. The upper, middle, and lower entries correspond to (a), (b), and (c), respectively.

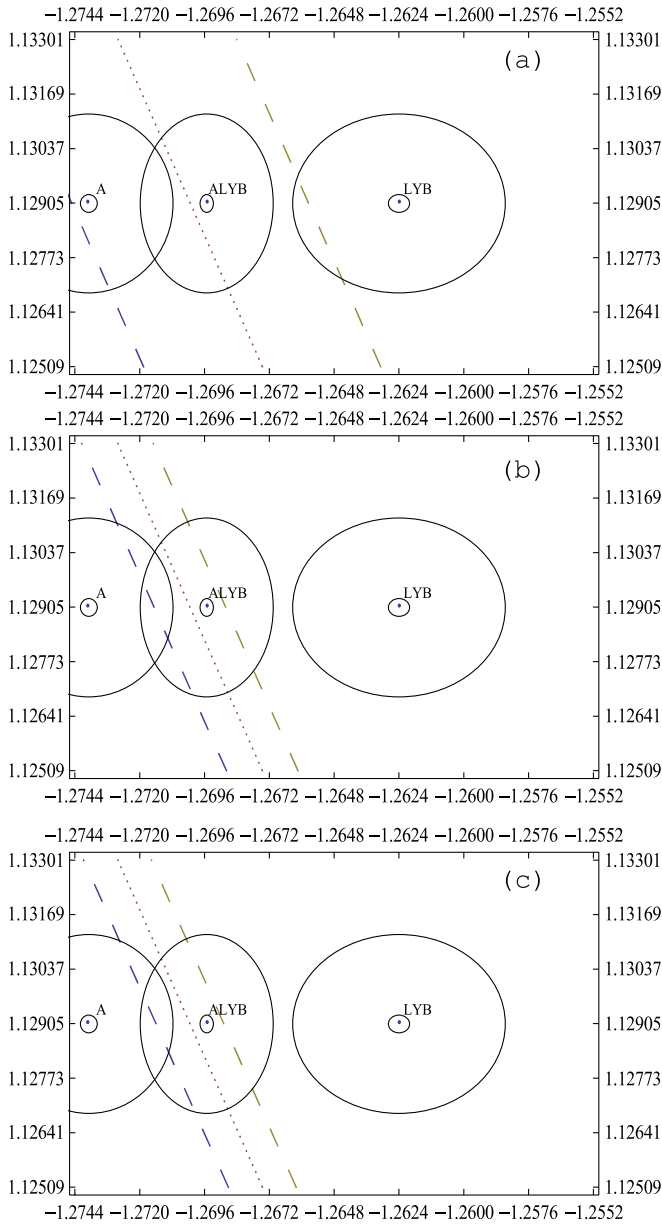


FIG. 2 (color online). The detailed numerical results corresponding to Table II are plotted here. The upper, middle, and lower entries correspond to (a), (b), and (c), respectively.

effective standard deviations above and below the central value of $R = 1.12905 \times 10^{-3} \text{ s}^{-1}$.

To study the effect of V_{us} upon the SMR we shall let its central value vary up to 3 standard deviations $\sigma_{V_{us}} = 0.0021$ above and below its current central value $V_{us} = 0.2257$. The other three restrictions in (6) will be kept fixed at their current experimental values.

There is no need to present all the details of our numerical analysis. Our results are well illustrated by exhibiting three cases for the central value of V_{us} , namely, 0.2194, 0.2257, and 0.2320 (the first one corresponds to the previous value of V_{us} , the second one to its current value, and the third one allows for still another three-sigma increase

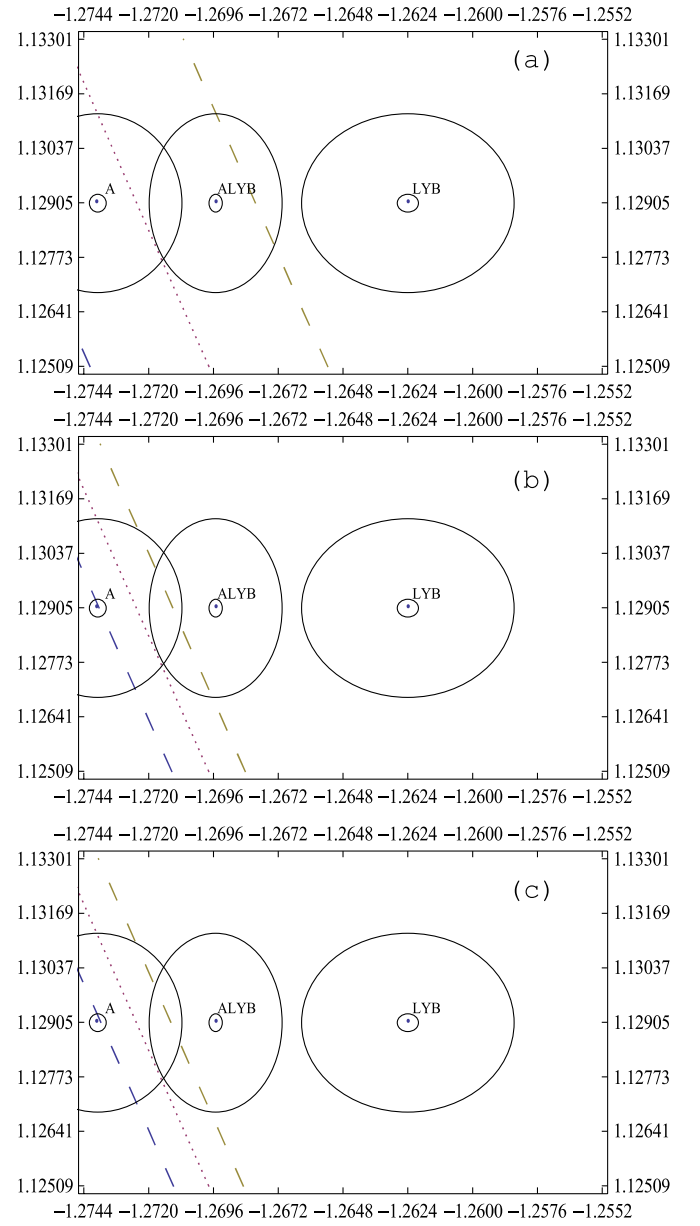


FIG. 3 (color online). The detailed numerical results corresponding to Table III are plotted here. The upper, middle, and lower entries correspond to (a), (b), and (c), respectively.

of V_{us}). In each of these cases we use the liberty we have to choose the size of $\sigma_{R'}$ and $\sigma_{\lambda'}$. The first choice for them is the corresponding experimental error bars 0.00132 and 0.0024. The resulting SMR could well be referred to as the “experimental” SMR. The second choice is to use one-tenth of these values, which as discussed in the last section is the theoretical SMR. And for the purpose of further discussion we use as a third choice one-hundredth of such values.

Our numerical results are given in Tables I, II, and III. The rows correspond to steps of 1 standard deviation in R' , λ_0 gives the corresponding position of the minimum χ_0^2 , and the 90% CL ranges of λ' are given in the column

TABLE IV. Values of χ^2 at sample points in the (λ, R) plane, corresponding to Table I. The upper, middle, and lower entries have the same meaning as in this table.

$R'(10^{-3} \text{ s}^{-1}) \backslash \lambda'$	-1.2744	-1.2720	-1.2696	-1.2672	-1.2648	-1.2624	-1.2600	-1.2576	-1.2552
1.125 09	14.82	9.43	5.67	3.52	3.00	4.10	6.82	11.17	17.14
	127.66	72.82	32.96	9.31	3.25	16.31	50.21	106.90	188.54
	139.40	79.79	36.14	10.03	3.28	18.02	56.75	122.43	218.63
1.126 41	12.60	7.81	4.65	3.11	3.18	4.89	8.21	13.16	19.73
	105.46	56.10	22.15	4.89	5.75	26.35	68.46	134.12	225.60
	115.31	61.51	24.22	5.11	6.10	29.43	77.78	154.30	262.84
1.127 73	10.61	6.43	3.86	2.92	3.60	5.90	9.83	15.38	22.56
	85.29	41.55	13.67	2.98	10.99	39.35	89.94	164.86	266.52
	93.36	45.56	14.86	2.99	12.00	44.28	102.65	190.52	312.02
1.129 05	8.86	5.27	3.31	2.97	4.24	7.15	11.68	17.83	25.61
	67.19	29.23	7.59	3.67	19.03	55.40	114.73	199.24	311.41
	73.63	32.02	8.12	3.77	21.11	62.70	131.55	231.30	366.41
1.130 37	7.34	4.35	2.99	3.24	5.12	8.63	13.76	20.51	28.90
	51.22	19.19	3.98	7.03	29.96	74.59	142.95	237.36	360.42
	56.16	20.96	4.11	7.54	33.55	84.84	164.63	276.85	426.31
1.131 69	6.05	3.66	2.89	3.75	6.23	10.34	16.07	23.43	32.41
	37.43	11.51	2.90	13.13	43.87	97.02	174.71	279.35	413.67
	41.04	12.46	2.90	14.42	49.45	110.86	202.10	327.41	492.01
1.133 01	4.99	3.20	3.03	4.49	7.57	12.28	18.61	26.57	36.16
	25.88	6.22	4.42	22.04	60.83	122.78	210.11	325.34	471.33
	28.33	6.60	4.61	24.53	68.94	140.91	244.16	383.24	563.83

headed by λ' . In each case the SMR is a band. This can be visualized in the corresponding Figs. 1–3.

To appreciate the variation of χ^2 within the rectangle in the (λ, R) plane we list its value at sample points in

Tables IV, V, and VI. In these tables one can see how the SMR is narrowed as $\sigma_{R'}$ and $\sigma_{\lambda'}$ are reduced from their experimental values to one-tenth of them. But one also sees

TABLE V. Values of χ^2 at sample points in the (λ, R) plane, corresponding to Table II. The upper, middle, and lower entries have the same meaning as in this table.

$R'(10^{-3} \text{ s}^{-1}) \backslash \lambda'$	-1.2744	-1.2720	-1.2696	-1.2672	-1.2648	-1.2624	-1.2600	-1.2576	-1.2552
1.125 09	9.64	5.78	3.54	2.91	3.90	6.50	10.71	16.55	24.00
	71.89	33.20	9.82	3.01	14.14	44.77	96.62	171.64	272.01
	78.36	36.21	10.55	3.02	15.49	50.14	109.54	196.75	315.44
1.126 41	8.01	4.75	3.11	3.08	4.66	7.86	12.68	19.11	27.16
	55.70	22.61	5.26	4.97	23.16	61.46	121.66	205.79	316.13
	60.76	24.60	5.52	5.20	25.65	69.16	138.48	236.86	368.27
1.127 73	6.61	3.95	2.91	3.48	5.66	9.48	14.87	21.91	30.56
	41.58	14.23	3.08	9.49	34.96	81.16	149.97	243.51	364.16
	45.36	15.40	3.10	10.24	38.99	91.72	171.38	281.45	426.20
1.129 05	5.45	3.38	2.94	4.10	6.88	11.28	17.30	24.93	34.19
	29.58	8.12	3.35	16.65	49.61	103.95	181.65	284.90	416.21
	32.24	8.67	3.40	18.31	55.63	117.96	208.41	330.73	489.51
1.130 37	4.51	3.05	3.20	4.96	8.34	13.34	19.95	28.19	38.04
	19.74	4.34	6.12	26.52	67.19	129.93	216.79	330.09	472.41
	21.45	4.50	6.49	29.44	75.69	148.02	249.75	384.91	558.47
1.131 69	3.81	2.94	3.69	6.05	10.03	15.62	22.84	31.67	42.13
	12.12	2.95	11.46	39.18	87.78	159.19	255.52	379.19	532.91
	13.07	2.95	12.47	43.76	99.30	182.06	295.60	444.25	633.39
1.133 01	3.33	3.06	4.41	7.37	11.94	18.14	25.95	35.39	46.44
	6.77	4.00	19.45	54.69	111.49	191.82	297.93	432.33	597.85
	7.14	4.12	21.44	61.36	126.61	220.27	346.17	509.01	714.63

TABLE VI. Values of χ^2 at sample points in the (λ, R) plane, corresponding to Table III. The upper, middle, and lower entries have the same meaning as in this table.

$R'(10^{-3} \text{ s}^{-1}) \setminus \lambda'$	-1.2744	-1.2720	-1.2696	-1.2672	-1.2648	-1.2624	-1.2600	-1.2576	-1.2552
1.125 09	5.87	3.58	2.90	3.82	6.34	10.48	16.22	23.57	32.53
	32.54	9.91	2.94	12.87	41.11	89.20	158.89	252.12	371.07
	35.31	10.61	2.95	13.99	45.67	100.23	180.31	289.04	430.22
1.126 41	4.85	3.15	3.06	4.58	7.70	12.43	18.77	26.72	36.28
	22.34	5.43	4.61	21.19	56.61	112.51	190.68	293.15	422.22
	24.20	5.68	4.79	23.28	63.18	126.87	217.16	337.40	491.66
1.127 73	4.05	2.95	3.46	5.57	9.29	14.62	21.56	30.11	40.27
	14.25	3.20	8.70	32.11	74.93	138.86	225.78	337.80	477.30
	15.35	3.22	9.33	35.52	83.95	157.14	258.08	390.36	558.36
1.129 05	3.49	2.99	4.09	6.80	11.11	17.04	24.57	33.72	44.48
	8.30	3.27	15.27	45.70	96.15	168.35	264.29	386.16	536.45
	8.83	3.31	16.65	50.83	108.12	191.19	303.24	448.13	630.57
1.130 37	3.16	3.25	4.95	8.25	13.16	19.68	27.82	37.56	48.92
	4.56	5.72	24.39	62.05	120.34	201.07	306.31	438.37	599.80
	4.72	6.01	26.85	69.32	135.80	229.17	352.84	510.95	708.59
1.131 69	3.05	3.74	6.03	9.93	15.44	22.56	31.29	41.63	53.56
	3.08	10.58	36.12	81.22	147.58	237.12	351.96	494.51	667.49
	3.08	11.42	40.02	91.07	167.13	271.25	407.07	579.06	792.75
1.133 01	3.18	4.46	7.35	11.84	17.95	25.66	34.99	45.93	58.48
	3.91	17.94	50.54	103.30	177.98	276.58	401.33	554.75	739.65
	4.00	19.62	56.26	116.23	202.26	317.60	466.15	652.74	883.38

that reducing them further produces no significant narrowing any more.

For comparison purposes, we include in Figs. 1–3, the 90% CL region around the central values of the current measurements and, also, the same regions at one-tenth of the present error bars. Although the effect of changing V_{us} is perceptible for the “experimental” SMR in Figs. 1(a),

2(a), and 3(a), it does not lead to sharp conclusions, unless V_{us} were to reach 0.2320. In contrast, the theoretical SMR of Figs. 1(b), 2(b), and 3(b) clearly discriminates λ_A and λ_{LYB} . The current situation is depicted in Fig. 2(b). λ_{LYB} is sharply incompatible with the SM. Thus, either the SM is quite accurate and λ_{LYB} will be eliminated or, if this λ_{LYB} is confirmed in the future, $n\beta d$ will produce strong evi-

TABLE VII. In the top part we give the individual contributions to χ^2 of Eq. (6) and total χ^2 at the border points of the 90% CL ranges of λ of the middle row of Table II. The upper, middle, and lower entries in each row have the same meaning as in this table. In the lower part we assume that σ_R and σ_λ are cut to 1/2, 1/5, and 1/7 and correspond to the second, third, and fourth entries in each row.

λ'	$\chi^2(R')$	$\chi^2(\lambda')$	$\chi^2(V_{us})$	$\chi^2(B_0)$	$\chi^2(a_0)$	$\chi^2(V_{ub})$	χ^2
-1.274 52	0.292 17	2.177 52	0.215 57	2.591 59	0.320 58	10^{-6}	5.597 43
-1.271 47	0.031 95	0.232 17	2.407 86	2.568 71	0.352 76	0.000 02	5.593 47
-1.271 40	0.000 35	0.002 57	2.665 90	2.565 82	0.356 94	0.000 02	5.591 60
-1.265 75	0.305 45	2.179 91	0.220 51	2.696 56	0.193 60	10^{-6}	5.596 03
-1.268 82	0.034 32	0.246 72	2.425 58	2.718 15	0.171 60	0.000 02	5.596 39
-1.268 89	0.000 38	0.002 75	2.701 12	2.721 18	0.168 62	0.000 02	5.594 08
-1.274 52	0.292 17	2.177 52	0.215 57	2.591 59	0.320 58	10^{-6}	5.597 43
-1.272 59	0.237 56	1.740 66	0.706 08	2.590 12	0.322 59	10^{-5}	5.597 02
-1.271 66	0.098 91	0.719 64	1.856 38	2.575 25	0.343 39	10^{-5}	5.593 60
-1.271 54	0.059 25	0.430 72	2.184 60	2.571 29	0.349 04	0.000 02	5.594 92
-1.271 47	0.031 95	0.232 17	2.407 86	2.568 71	0.352 76	0.000 02	5.593 47
-1.265 75	0.305 45	2.179 91	0.220 51	2.696 56	0.193 60	10^{-6}	5.596 03
-1.267 69	0.245 71	1.759 02	0.704 65	2.697 05	0.193 07	10^{-5}	5.599 51
-1.268 64	0.104 40	0.749 83	1.851 93	2.711 46	0.178 27	10^{-5}	5.595 91
-1.268 76	0.063 21	0.454 21	2.192 25	2.715 50	0.174 22	0.000 02	5.599 42
-1.268 82	0.034 32	0.246 72	2.425 58	2.718 15	0.171 60	0.000 02	5.596 39

dence for not too far away new physics. Correspondingly, if λ_A is confirmed in the future, the accuracy of the SM will be sustained and new physics will be further away; so it will be harder to detect it in $n\beta d$. The above disjunctive is further strengthened if V_{us} is measured still higher, as seen in Fig. 3(b). Notice that the current central values of λ_A and λ_{LYB} , if either of them were to be confirmed, strongly indicate the existence of new physics, as can be appreciated with the small regions around them in Fig. 2(b). The SM would remain very accurate if λ_A were confirmed and V_{us} were further increased up to 0.2320. This possibility is illustrated in Fig. 3(c). Surprisingly, the inconsistent average λ_{ALYB} is fully compatible with the SM at present, as seen in Fig. 2(b).

That arbitrarily reducing $\sigma_{R'}$ and $\sigma_{\lambda'}$ up to one-hundredth of their experimental counterparts produced no significant reduction of the SMR, as can be seen in Figs. 1(c), 2(c), and 3(c), requires some detailed discussion. The reason for this can be traced to the individual contributions of R' , λ' , and V_{us} to χ^2 of Eq. (6). In this respect, we have produced Table VII. It is sufficient to present the case of the central row in Table II, where $V_{us} = V_{us}^{\text{exp}} = 0.2257$ and $R = R^{\text{exp}} = 1.12905 \times 10^{-3} \text{ s}^{-1}$, and the contributions to χ^2 at the border of the SMR, namely, the extremes of the corresponding ranges of λ' in Table II.

In the top part of Table VII we give the six different contributions to χ^2 at the above extremes. One can see that with $\sigma_{R'}$ and $\sigma_{\lambda'}$ at their experimental values the $\chi^2(R')$ and $\chi^2(\lambda')$ contributions dominate over the $\chi^2(V_{us})$ contribution (upper entries). At 1/10 of these values the situation is reversed, and it remains so when $\sigma_{R'}$ and $\sigma_{\lambda'}$ are reduced up to 1/100 (second and third entries). In the lower part of Table VII we trace in more detail when this reversal takes place by reducing $\sigma_{R'}$ and $\sigma_{\lambda'}$ by 1/2, 1/5, and 1/7 (second, third, and fourth entries, respectively). The dominance of $\chi^2(V_{us})$ over $\chi^2(R')$ and $\chi^2(\lambda')$ takes place already when $\sigma_{R'}$ and $\sigma_{\lambda'}$ are cut to between 1/4 and 1/5 of their experimental counterparts. Notice that this reversal does not depend on B_0 , a_0 , and V_{ub} , whose χ^2 contributions remain fairly constant throughout Table VII. One may conclude that the potential of the SM prediction at 1/10 of the experimental errors on R and λ cannot be reached, because of the current uncertainty on V_{us} . In other words, even if the experimental precision in $n\beta d$ were to be greatly improved in the near future, the comparison with the SM predictions will be severely limited by the experimental precision of V_{us} .

Let us next study in detail the effects of improving the precision of V_{us} .

IV. THE PRECISION OF V_{us} AND THE STANDARD MODEL REGION

$n\beta d$ cannot provide a better test of the SM even if the error bars on R and λ and the theoretical uncertainty in Eq. (1) were to be reduced beyond one-fifth. As seen in the

TABLE VIII. This table corresponds to Table I, except that now it is assumed that $\sigma_{V_{us}}$ is cut to 1/10, namely, $\sigma_{V_{us}} = 0.00021$.

R'	χ_0^2	λ_0	λ'
1.125 09	2.974 83	-1.265 21	(-1.269 42, -1.261 00)
	2.975 22	-1.265 20	(-1.265 63, -1.264 76)
	2.975 23	-1.265 20	(-1.265 32, -1.265 07)
1.126 41	2.939 50	-1.266 11	(-1.270 32, -1.261 90)
	2.939 74	-1.266 09	(-1.266 53, -1.265 65)
	2.939 74	-1.266 09	(-1.266 22, -1.265 96)
1.127 73	2.913 64	-1.267 00	(-1.271 21, -1.262 79)
	2.913 75	-1.266 99	(-1.267 43, -1.266 55)
	2.913 75	-1.266 99	(-1.267 12, -1.266 86)
1.129 05	2.897 18	-1.267 89	(-1.272 10, -1.263 68)
	2.897 21	-1.267 88	(-1.268 32, -1.267 45)
	2.897 21	-1.267 88	(-1.268 01, -1.267 75)
1.130 37	2.890 05	-1.268 78	(-1.272 99, -1.264 57)
	2.890 05	-1.268 78	(-1.269 22, -1.268 34)
	2.890 05	-1.268 78	(-1.268 91, -1.268 65)
1.131 69	2.892 21	-1.269 67	(-1.273 88, -1.265 46)
	2.892 22	-1.269 67	(-1.270 11, -1.269 23)
	2.892 22	-1.269 67	(-1.269 80, -1.269 54)
1.133 01	2.903 58	-1.270 56	(-1.274 77, -1.266 35)
	2.903 64	-1.270 56	(-1.271 00, -1.270 13)
	2.903 64	-1.270 56	(-1.270 69, -1.270 44)

previous section, the limitation comes from the error bars on V_{us} . The central value of V_{us} does shift the position of the SMR, but it is reducing $\sigma_{V_{us}}$ that will improve the width of the SMR.

TABLE IX. This table corresponds to Table II, except that now it is assumed that $\sigma_{V_{us}}$ is cut to 1/10, namely, $\sigma_{V_{us}} = 0.00021$.

R'	χ_0^2	λ_0	λ'
1.125 09	2.903 94	-1.267 46	(-1.271 67, -1.263 25)
	2.904 00	-1.267 45	(-1.267 89, -1.267 01)
	2.904 02	-1.267 45	(-1.267 59, -1.267 32)
1.126 41	2.892 30	-1.268 35	(-1.272 56, -1.264 14)
	2.892 31	-1.268 35	(-1.268 79, -1.267 91)
	2.892 31	-1.268 35	(-1.268 48, -1.268 22)
1.127 73	2.890 03	-1.269 25	(-1.273 46, -1.265 04)
	2.890 03	-1.269 25	(-1.269 69, -1.268 81)
	2.890 09	-1.269 25	(-1.269 38, -1.269 11)
1.129 05	2.897 05	-1.270 14	(-1.274 35, -1.265 93)
	2.897 09	-1.270 14	(-1.270 58, -1.269 70)
	2.897 10	-1.270 14	(-1.270 27, -1.270 01)
1.130 37	2.913 33	-1.271 03	(-1.275 24, -1.266 82)
	2.913 44	-1.271 04	(-1.271 48, -1.270 60)
	2.913 50	-1.271 04	(-1.271 17, -1.270 91)
1.131 69	2.938 78	-1.271 92	(-1.276 13, -1.267 71)
	2.939 01	-1.271 93	(-1.272 37, -1.271 49)
	2.939 03	-1.271 93	(-1.272 07, -1.271 80)
1.133 01	2.973 36	-1.272 81	(-1.277 02, -1.268 60)
	2.973 75	-1.272 83	(-1.273 27, -1.272 39)
	2.973 80	-1.272 83	(-1.272 96, -1.272 69)

TABLE X. This table corresponds to Table III, except that now it is assumed that $\sigma_{V_{us}}$ is cut to 1/10, namely, $\sigma_{V_{us}} = 0.00021$.

R'	χ_0^2	λ_0	λ'
1.125 09	2.893 11	-1.269 78	(-1.273 99, -1.265 57)
	2.893 13	-1.269 78	(-1.270 22, -1.269 34)
	2.893 14	-1.269 78	(-1.269 92, -1.269 65)
1.126 41	2.905 72	-1.270 67	(-1.274 88, -1.266 46)
	2.905 72	-1.270 67	(-1.271 12, -1.270 24)
	2.905 87	-1.270 68	(-1.270 82, -1.270 54)
1.127 73	2.927 60	-1.271 57	(-1.275 78, -1.267 36)
	2.927 78	-1.271 58	(-1.272 02, -1.271 14)
	2.927 91	-1.271 58	(-1.271 71, -1.271 44)
1.129 05	2.958 68	-1.272 46	(-1.276 67, -1.268 25)
	2.959 00	-1.272 48	(-1.272 92, -1.272 03)
	2.959 05	-1.272 48	(-1.272 61, -1.272 34)
1.130 37	2.998 90	-1.273 35	(-1.277 56, -1.269 14)
	2.999 41	-1.273 37	(-1.273 81, -1.272 93)
	2.999 42	-1.273 37	(-1.273 51, -1.273 24)
1.131 69	3.048 22	-1.274 24	(-1.278 45, -1.270 03)
	3.048 94	-1.274 27	(-1.274 71, -1.273 83)
	3.048 97	-1.274 27	(-1.274 41, -1.274 13)
1.133 01	3.106 56	-1.275 14	(-1.279 35, -1.270 93)
	3.107 54	-1.275 16	(-1.275 60, -1.274 72)
	3.107 60	-1.275 16	(-1.275 30, -1.275 03)

To see this we have reproduced the SMR assuming $\sigma_{V_{us}}$ is cut to one-tenth of its current value, that is, $\sigma_{V_{us}} = 0.00021$, and assuming the central value to be at three places, $V_{us} = 0.2194, 0.2257, \text{ or } 0.2320$. Of course this last

is only an assumption; all we can say as of now is that such a central value will fall at 90% CL somewhere within the band of Fig. 2(b). The corresponding numerical results are summarized in Tables VIII, IX, and X for χ_0^2 , λ_0 , and the 90% CL range of λ' . Values of χ^2 at sample points in the (λ, R) plane are found in Tables XI, XII, and XIII. In each row of these six tables the upper, middle, and lower entries correspond to $\sigma_{R'}$ and $\sigma_{\lambda'}$ at σ_R and σ_λ , at $\sigma_R/10$ and $\sigma_\lambda/10$, and at $\sigma_R/100$ and $\sigma_\lambda/100$, respectively. Notice that the numerical values of χ_0^2 and λ_0 are practically the same in Tables I and VIII, II and IX, and III and X. The minimum of χ^2 and the position of the minimum in the (λ, R) plane are practically independent of the values of $\sigma_{R'}$, $\sigma_{\lambda'}$, and $\sigma_{V_{us}}$. In contrast, the values of χ^2 at sample points in the (λ, R) plane away from the SMR become enormous, as can be appreciated looking throughout Tables XI, XII, and XIII. Such increases in χ^2 indicate the substantial narrowing of the SMR as $\sigma_{V_{us}}$ is reduced along with $\sigma_{R'}$ and $\sigma_{\lambda'}$. These results can be visualized in Figs. 4–6. Comparing these last figures with the corresponding ones of Sec. III, one sees that the “experimental” SMR is not noticeably reduced, as was to be expected. However, at one-tenth $\sigma_{R'}$ and $\sigma_{\lambda'}$, the comparison of Figs. 1(b), 2(b), and 3(b) with Figs. 4(b), 5(b), and 6(b), respectively, shows that the effect of reducing $\sigma_{V_{us}}$ is quite impressive. As seen in Tables XI, XII, and XIII, the SMR is greatly reduced. This reduction of the SMR could lead to almost a thin line if the theoretical and experimental uncertainties in R and λ were put under much better control, as can be visualized in Figs. 4(c), 5(c), and 6(c).

TABLE XI. This table corresponds to Table IV, except that now it is assumed that $\sigma_{V_{us}}$ is cut to 1/10, namely, $\sigma_{V_{us}} = 0.00021$.

$R'(10^{-3} \text{ s}^{-1}) \setminus \lambda'$	-1.2744	-1.2720	-1.2696	-1.2672	-1.2648	-1.2624	-1.2600	-1.2576	-1.2552
1.125 09	15.83	9.99	5.90	3.58	3.00	4.18	7.12	11.80	18.25
	1193.11	653.49	275.56	59.42	5.18	112.94	382.79	814.84	1409.18
	12 460.00	6988.55	3008.19	642.41	28.65	1320.42	4689.62	10 329.40	18 457.20
1.126 41	13.42	8.23	4.80	3.12	3.20	5.03	8.62	13.96	21.06
	972.71	493.42	175.88	20.18	26.44	194.73	525.18	1017.87	1672.91
	10 241.20	5316.84	1927.06	200.14	279.14	2323.96	6513.91	13 050.60	22 161.40
1.127 73	11.26	6.73	3.95	2.92	3.65	6.13	10.37	16.37	24.12
	774.96	355.99	98.82	3.54	70.27	299.09	690.12	1243.44	1959.15
	8224.81	3862.50	1079.81	10.20	802.58	3623.61	8660.38	16 123.40	26 250.40
1.129 05	9.36	5.47	3.34	2.97	4.35	7.49	12.38	19.03	27.43
	599.83	241.16	44.34	9.46	136.64	425.97	877.56	1491.49	2267.86
	6415.87	2630.99	472.56	79.42	1606.66	5228.04	11 138.80	19 559.00	30 737.00
1.130 37	7.71	4.47	2.99	3.27	5.30	9.09	14.63	21.93	30.99
	447.28	148.89	12.40	37.91	225.53	575.35	1087.47	1761.99	2599.01
	4819.44	1627.99	111.66	414.94	2699.41	7146.31	13 959.50	23 368.80	35 634.30
1.131 69	6.30	3.72	2.89	3.82	6.51	10.95	17.14	25.09	34.80
	317.26	79.14	2.96	88.84	336.88	747.17	1319.81	2054.91	2952.55
	3440.83	859.42	3.73	1024.18	4089.20	9387.86	17 133.10	27 565.20	40 956.00
1.133 01	5.15	3.22	3.04	4.62	7.96	13.05	19.90	28.50	38.86
	209.76	31.88	16.00	162.23	470.67	941.41	1574.55	2370.20	3328.45
	2285.50	331.40	155.64	1914.89	5784.74	11 962.50	20 670.70	32 160.60	46 716.70

TABLE XII. This table corresponds to Table V, except that now it is assumed that $\sigma_{V_{us}}$ is cut to 1/10, namely, $\sigma_{V_{us}} = 0.00021$.

$R'(10^{-3} \text{ s}^{-1}) \setminus \lambda'$	-1.2744	-1.2720	-1.2696	-1.2672	-1.2648	-1.2624	-1.2600	-1.2576	-1.2552
1.125 09	10.24	6.04	3.60	2.91	3.98	6.80	11.38	17.70	25.78
	677.51	292.00	67.39	3.79	101.31	360.05	780.13	1361.63	2104.68
	6885.08	3027.71	695.41	12.72	1118.13	4166.06	9329.22	16 801.30	26 800.00
1.126 41	8.46	4.92	3.13	3.09	4.81	8.29	13.52	20.50	29.23
	514.57	189.18	24.75	21.38	179.19	498.27	978.73	1620.68	2424.23
	5267.30	1969.07	239.73	208.68	2019.96	5834.38	11 832.00	20 214.80	31 210.20
1.127 73	6.94	4.05	2.91	3.53	5.90	10.03	15.91	23.54	32.93
	374.19	108.91	4.64	61.48	279.55	658.96	1199.79	1902.17	2766.19
	3855.82	1131.72	21.99	661.14	3199.04	7803.19	14 661.30	23 984.30	36 009.60
1.129 05	5.66	3.43	2.94	4.21	7.24	12.02	18.55	26.84	36.88
	256.34	51.14	7.02	124.06	402.38	842.09	1443.28	2206.07	3130.55
	2655.59	521.18	48.36	1376.99	4663.08	10 081.20	17 827.00	28 120.90	41 210.90
1.130 37	4.64	3.06	3.22	5.15	8.82	14.26	21.44	30.38	41.08
	160.97	15.85	31.85	209.07	547.63	1047.62	1709.15	2532.33	3517.26
	1671.75	143.16	325.22	2363.39	6420.14	12 677.40	21 339.52	32 636.20	46 827.20
1.131 69	3.88	2.94	3.76	6.33	10.66	16.75	24.59	34.18	45.53
	88.07	3.00	79.11	316.49	715.26	1275.52	1997.37	2880.92	3926.27
	909.64	3.62	859.21	3627.80	8478.60	15 601.30	25 209.20	37 542.40	52 872.10
1.133 01	3.36	3.07	4.54	7.77	12.75	19.49	27.98	38.23	50.23
	37.58	12.55	148.75	446.27	905.24	1525.75	2307.91	3251.81	4357.57
	374.79	108.74	1657.27	5177.98	10 847.20	18 862.80	29 447.40	42 852.00	59 360.20

There is a systematic feature in Tables I, II, and III and VIII, IX, and X: the value of χ_0^2 is always around 2.90. The reason for this is found in Table VII: the contribution of the neutrino asymmetry B_0 to χ^2 is always around 2.70. This is 1.6 standard deviations from the SM

prediction. It is not significant, and we shall not discuss it further.

It is clear that the ability of $n\beta d$ to test the SM is intimately connected with the precision to determine V_{us} in strangeness-changing decays.

TABLE XIII. This table corresponds to Table VI, except that now it is assumed that $\sigma_{V_{us}}$ is cut to 1/10, namely, $\sigma_{V_{us}} = 0.00021$.

$R'(10^{-3} \text{ s}^{-1}) \setminus \lambda'$	-1.2744	-1.2720	-1.2696	-1.2672	-1.2648	-1.2624	-1.2600	-1.2576	-1.2552
1.125 09	6.14	3.64	2.90	3.91	6.67	11.18	17.44	25.46	35.24
	299.31	71.28	3.35	95.64	348.25	761.30	1334.90	2069.16	2964.19
	2951.38	700.34	7.72	999.09	3813.89	8607.42	15 553.10	24 845.10	36 701.30
1.126 41	5.02	3.17	3.08	4.74	8.16	13.32	20.24	28.92	39.34
	195.23	27.11	19.15	171.45	484.14	957.31	1591.10	2385.60	3340.92
	1932.00	251.88	174.37	1829.89	5363.41	10 936.60	18 730.00	28 946.10	41 812.50
1.127 73	4.15	2.96	3.52	5.83	9.90	15.72	23.29	32.62	43.70
	113.63	5.40	57.38	269.69	642.43	1175.72	1869.67	2724.40	3740.00
	1122.64	28.56	582.94	2921.28	7194.36	13 570.40	22 237.80	33 407.50	47 317.20
1.129 05	3.53	2.99	4.20	7.17	11.89	18.37	26.60	36.58	48.31
	54.46	6.11	118.02	390.31	823.09	1416.48	2170.58	3085.51	4161.37
	528.29	35.93	1239.62	4280.18	9314.50	16 517.80	26 086.30	38 240.40	53 227.90
1.130 37	3.17	3.28	5.14	8.76	14.14	21.27	30.15	40.78	53.17
	17.69	29.20	201.02	533.28	1026.09	1679.56	2493.79	3468.91	4605.00
	154.13	279.75	2150.84	5913.79	11 731.90	19 787.70	30 285.80	43 456.20	59 557.70
1.131 69	3.05	3.82	6.33	10.61	16.63	24.41	33.95	45.24	58.28
	3.29	74.64	306.36	698.57	1251.39	1964.91	2839.26	3874.55	5070.87
	5.55	766.02	3323.28	7829.59	14 454.90	23 389.60	34 846.90	49 067.00	66 320.30
1.133 01	3.19	4.60	7.77	12.70	19.38	27.81	38.00	49.95	63.64
	11.22	142.39	433.99	886.14	1498.94	2272.51	3206.96	4302.40	5558.92
	88.11	1500.95	4763.89	10 035.40	17 492.40	27 333.30	39 780.70	55 085.40	73 529.80

V. PREDICTIONS OF V_{us} FROM NEUTRON BETA DECAY

A precise determination of V_{us} in strangeness-changing decays may take longer than precise measurements of R and α_e or λ . $n\beta d$ may provide a better determination of V_{us} via the unitarity of the CKM matrix, once the former produces a precise measurement of V_{ud} . This is a complementary way to appreciate the results of the last two sections.

First, let us look into the current determination of V_{ud} . The ambiguity in λ leads to an ambiguity in the experimental value of V_{ud} . One has correspondingly two incompatible values for V_{ud} , namely,

$$V_{ud}^{\text{LYB}} = 0.9791 \pm 0.0016 \quad (7)$$

and

$$V_{ud}^{\text{A}} = 0.9718 \pm 0.0013. \quad (8)$$

One may also quote the third, albeit inconsistent, value

$$V_{ud}^{\text{ALYB}} = 0.9746 \pm 0.0011. \quad (9)$$

Although not yet satisfactory, one can already see that the error bars are competitive with V_{ud} determined from other sources [1]. Also, within the validity of the SM, these values are accompanied by

$$V_{us}^{\text{LYB}} = 0.2032 \pm 0.0079, \quad (10)$$

$$V_{us}^{\text{A}} = 0.2357 \pm 0.0055, \quad (11)$$

and

$$V_{us}^{\text{ALYB}} = 0.2239 \pm 0.0048. \quad (12)$$

Again, even if not satisfactory, the error bars are becoming competitive with V_{us} determined from other sources [1].

Let us match Eqs. (10)–(12) with the value of V_{us} from K_{l3} decays (which was used in the previous sections), namely,

$$V_{us}^{K_{l3}} = 0.2257 \pm 0.0021. \quad (13)$$

It is convenient to produce the 90% CL ranges that correspond to these V_{us} values. They are

$$V_{us}^{\text{LYB}}(90\% \text{ CL}) = (0.1902, 0.2162), \quad (14)$$

$$V_{us}^{\text{A}}(90\% \text{ CL}) = (0.2267, 0.2447), \quad (15)$$

$$V_{us}^{\text{ALYB}}(90\% \text{ CL}) = (0.2160, 0.2318), \quad (16)$$

and

$$V_{us}^{K_{l3}}(90\% \text{ CL}) = (0.2223, 0.2291). \quad (17)$$

One can readily see that range (14) is below (17) and there is no overlap between them at all. Range (15) is above (17), and there is a small overlap between the two. Contrastingly, range (16) fully contains range (17). These

comparisons correspond to the overlapping or lack of it of the 90% CL ellipses with the SMR exhibited in Fig. 2(b).

Also, they indirectly exhibit the current experimental problem in the determination of λ . Ranges (14) and (15) do not overlap with one another and are quite separated. These comparisons are complementary to the analysis of Secs. III and IV. They provide a quick way to see the compatibility of $n\beta d$ data together with K_{l3} data with the SM assumptions.

The present experimental situation will be corrected eventually. In the meantime, we can extend this analysis through V_{us} . To appreciate what can be expected we have produced a set of values for V_{ud} and V_{us} assuming the central values of R and λ are at the left- and right-hand and at the center of the 90% CL ranges of λ_{LYB} , λ_{A} , and λ_{ALYB} . The former two are indicated by a $-$ and a $+$ sign, respectively. The corresponding error bars are $\sigma_R/10$ and $\sigma_\lambda/10$. These points and their 90% CL regions are displayed in Fig. 7. The numerical results are exhibited in Table XIV.

The main result that can be seen in this table is the size of the error bars of V_{ud} and V_{us} . $\sigma_{V_{ud}}$ is reduced to around 0.0002, which is between 1/5 and 1/6 of the error bars of Eqs. (7)–(9). $\sigma_{V_{us}}$ is reduced to around 0.0008, which is between 1/2 and 1/3 of the current error bar of 0.0021 of Eq. (13). Clearly, once $n\beta d$ produces a consistent value for V_{ud} its potential precision will improve substantially over its determination from other sources. Assuming CKM-matrix unitarity, its accompanying value for V_{us} will improve over its current determination from strangeness-changing decays and may remain so for some time. This value will be useful in calculations that assume the validity of the SM and in coming tests of the unitarity triangle. A direct comparison with the independently improved future determinations of V_{us} from strangeness-changing decays will readily indicate if signals of new physics are present or not.

VI. SUMMARY AND DISCUSSION

$n\beta d$ data and K_{l3} data are two sets of independent data, and each one by itself cannot test the SM. So it is not a question of whether the former is compatible with the latter. Only using the two sets simultaneously can provide tests on the SM and the question is if their simultaneous use is compatible with the SM assumptions. Such compatibility can be fully seen through the overlap of the 90% CL ellipses around precise experimental determinations of R and λ with the band of the SMR, which requires precise V_{us} determinations in strangeness-changing decays and, in particular, in K_{l3} decays. The nonoverlapping of these two regions would give signals of physics beyond the SM.

The current potential of $n\beta d$ to discover new physics is seen in the overlap of the 90% CL regions around λ_{A} and λ_{LYB} with the theoretical SMR in Fig. 2(b). The recent change of 3 standard deviations in V_{us} can be appreciated

in the shift of the SMR from Fig. 1(b) to Fig. 2(b). This shift is toward λ_A , meaning that λ_{LBY} is either ruled out by the accuracy of the SM or it gives a strong signal for new physics. In contrast, λ_A favors such an accuracy and, if confirmed in the future, it means that new physics is further away.

However, the current potential is limited by the experimental precision of V_{us} . Actually, if such precision is not improved, reducing the error bars on R and λ beyond 1/4 or 1/5 of their current values will not lead to better tests of the SM. However, if this precision is improved in the future to somewhere between 1/2 and 1/3 of what it is at present, then $n\beta d$ will provide tests of the SM at the level of the value of V_{us} it can produce, via CKM-matrix unitarity, as

can be appreciated from the combined analysis of Secs. III, IV, and V.

The full potential of the SMR to confirm the accuracy of the SM is seen when $\sigma_{V_{us}}$ is reduced further. If eventually strangeness-changing decays are to reduce $\sigma_{V_{us}}$ to 1/10 of its current value, then the SMR becomes a very thin band. This can be visualized in Figs. 4–6. When this occurs, $n\beta d$ combined with strangeness-changing decays will provide very severe tests of the SM and may detect new physics which for whatever reason is very far away.

Before the above situation occurs, $n\beta d$ may produce a prediction for V_{us} via the unitarity of the CKM matrix. Such a prediction may be useful, while the experimental V_{us} remains at its current value, in calculations that assume

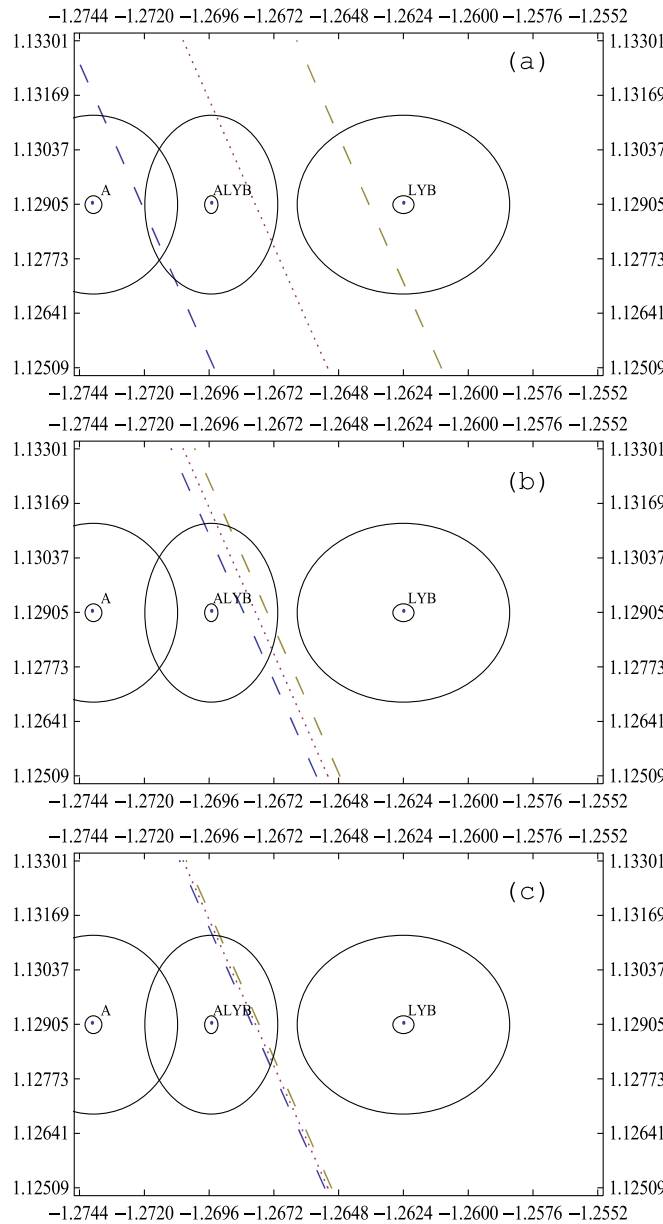


FIG. 4 (color online). These figures correspond to Figs. 1(a)–1(c) when $\sigma_{V_{us}}$ is assumed to be at 0.000 21.

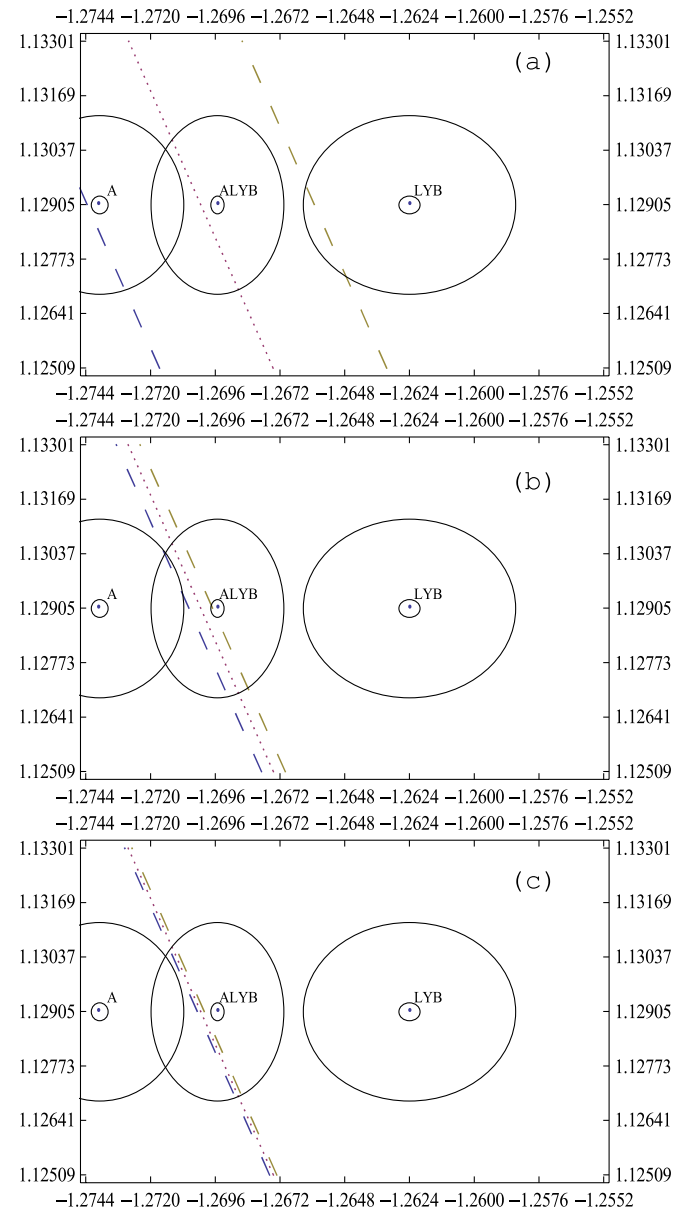


FIG. 5 (color online). These figures correspond to Figs. 2(a)–2(c) when $\sigma_{V_{us}}$ is assumed to be at 0.000 21.

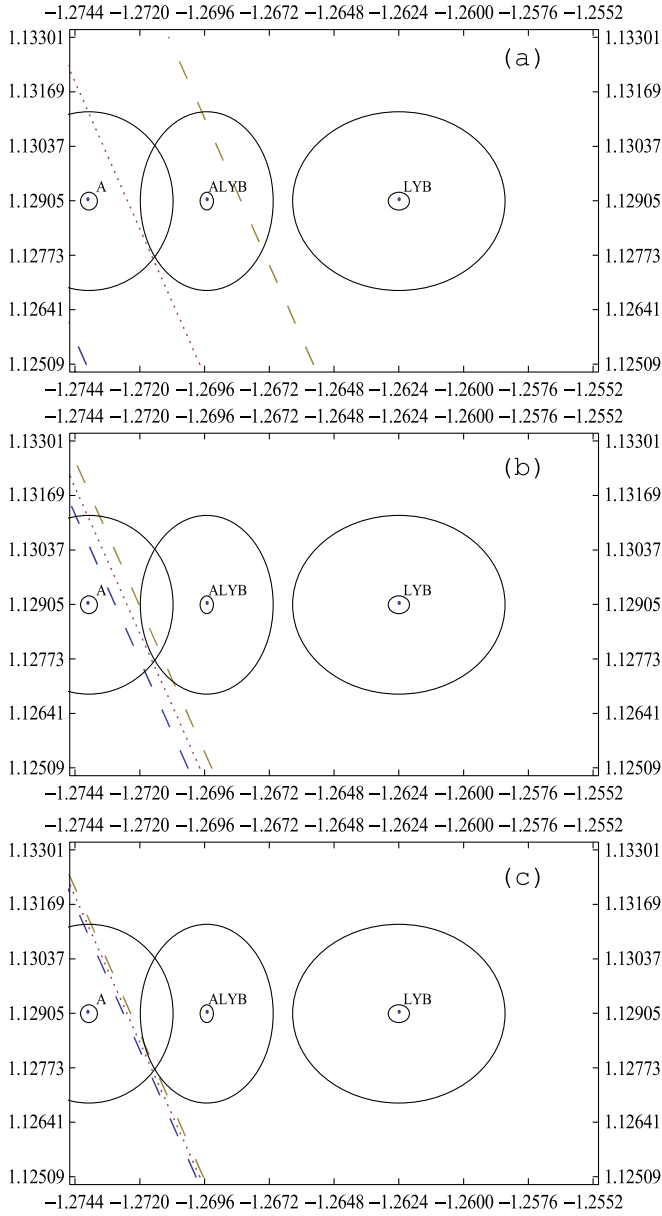


FIG. 6 (color online). These figures correspond to Figs. 3(a)–3(c) when $\sigma_{V_{us}}$ is assumed to be at 0.000 21.

the validity of the SM and in other tests of the SM through the unitarity triangle. Also, even if $n\beta d$ data are independent of K_{l3} data, this prediction of V_{us} with $n\beta d$ data may appear to be incompatible with the measurement of V_{us} in K_{l3} . This apparent incompatibility of $n\beta d$ and K_{l3} decays would provide a quick indication of the necessity to go beyond the SM.

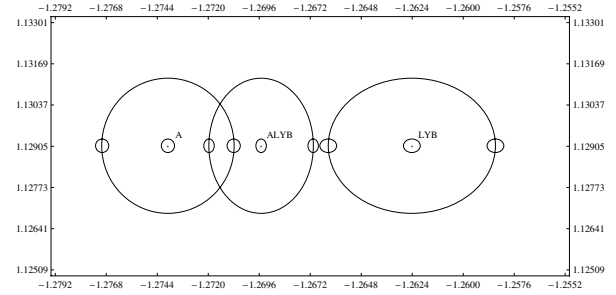


FIG. 7 (color online). Current 90% CL regions around λ_{LYB} , λ_A , and λ_{ALYB} and 90% CL regions around the central and horizontal border points when σ_R and σ_λ are cut to 1/10 of their present values.

TABLE XIV. Values of V_{ud} and V_{us} assuming the central values of R and λ are within the small regions displayed in Fig. 7. The $-$ and $+$ indices correspond to the left- and right-hand horizontal border points of each of the larger 90% CL regions in this figure.

λ	V_{ud}	V_{us}
$\lambda_A^- = -1.2770$	$0.969\,84 \pm 0.000\,20$	$0.243\,72 \pm 0.000\,78$
$\lambda_A = -1.2739$	$0.971\,80 \pm 0.000\,20$	$0.235\,75 \pm 0.000\,81$
$\lambda_A^+ = -1.2708$	$0.973\,78 \pm 0.000\,20$	$0.227\,45 \pm 0.000\,85$
$\lambda_{ALYB}^- = -1.2720$	$0.973\,03 \pm 0.000\,16$	$0.230\,62 \pm 0.000\,66$
$\lambda_{ALYB} = -1.2695$	$0.974\,60 \pm 0.000\,16$	$0.223\,93 \pm 0.000\,68$
$\lambda_{ALYB}^+ = -1.2670$	$0.976\,16 \pm 0.000\,16$	$0.216\,99 \pm 0.000\,70$
$\lambda_{LYB}^- = -1.2663$	$0.976\,61 \pm 0.000\,25$	0.2150 ± 0.0011
$\lambda_{LYB} = -1.2624$	$0.979\,13 \pm 0.000\,25$	0.2032 ± 0.0012
$\lambda_{LYB}^+ = -1.2585$	$0.981\,66 \pm 0.000\,25$	0.1906 ± 0.0013

Even if the present situation in $n\beta d$ is not satisfactory, ideally in the future the combined effort of reducing the theoretical and experimental error will produce a SMR close to a line, as can be seen in Figs. 4(c), 5(c), and 6(c). Difficult as this task may seem, it does show the potential low energy physics has to test the SM.

ACKNOWLEDGMENTS

One of us (G. S.-C.) is grateful to the Faculty of Mathematics, Autonomous University of Yucatán, Mexico, for hospitality where part of this work was done. A.G. and G. S.-C. would like to thank CONACyT (Mexico) for partial support.

[1] W.-M. Yao *et al.*, J. Phys. G **33**, 1 (2006).
[2] A review and original references are found in Ref. [1].

[3] A. García and J.L. García-Luna, Phys. Lett. B **546**, 247 (2002).

- [4] A. García, J.L. García-Luna, and G. López Castro, Phys. Lett. B **500**, 66 (2001).
- [5] W.J. Marciano and A. Sirlin, Phys. Rev. Lett. **56**, 22 (1986).
- [6] D.H. Wilkinson, Z. Phys. A **348**, 129 (1994).
- [7] A. Czarnecki, W.J. Marciano, and A. Sirlin, Phys. Rev. D **70**, 093006 (2004).
- [8] J.L. García-Luna and A. García, J. Phys. G **32**, 333 (2006).
- [9] H. Abele *et al.*, Phys. Rev. Lett. **88**, 211801 (2002).
- [10] P. Liaud, Nucl. Phys. **A612**, 53 (1997).
- [11] B. Yerozolimsky *et al.*, Phys. Lett. B **412**, 240 (1997).
- [12] P. Bopp *et al.*, Phys. Rev. Lett. **56**, 919 (1986).
- [13] This range covers 3 standard deviations $\sigma_\lambda = 0.0024$ above and 5 standard deviations below $\lambda_{\text{LYB}} = -1.2624$.